Published in final edited form as:
*Clin Cancer Res*. 2013 August 15; 19(16): 4422–4432. doi:10.1158/1078-0432.CCR-13-0788.

# Inhibition of protein phosphatase 2A radiosensitizes pancreatic cancers by modulating CDC25C/CDK1 and homologous recombination repair

**Dongping Wei**[1], **Leslie A. Parsels**[2], **David Karnak**[1], **Mary A. Davis**[1], **Joshua D. Parsels**[2], **Lili Zhao**[3], **Jonathan Maybaum**[2], **Theodore S. Lawrence**[1], **Yi Sun**[1], and **Meredith A. Morgan**[1]

[1]Department of Radiation Oncology, University of Michigan Medical School, Ann Arbor, MI 48109

[2]Department of Pharmacology, University of Michigan Medical School, Ann Arbor, MI 48109

[3]Department of Biostatistics, University of Michigan Comprehensive Cancer Center, Ann Arbor, MI 48109

## Abstract

**Purpose—**To identify targets whose inhibition may enhance the efficacy of chemoradiation in pancreatic cancer and thus improve survival, we performed an siRNA library screen in pancreatic cancer cells. We investigated PPP2R1A, a scaffolding subunit of protein phosphatase 2A (PP2A) as a lead radiosensitizing target.

**Experimental Design—**We determined the effect of PP2A inhibition by genetic (PPP2R1A siRNA) and pharmacological (LB100, a small molecule entering Phase I clinical trials) approaches on radiosensitization of Panc-1 and MiaPaCa-2 pancreatic cancer cells both *in vitro* and *in vivo*.

**Results—**PPP2R1A depletion by siRNA radiosensitized Panc-1 and MiaPaCa-2 cells, with radiation enhancement ratios of 1.4 ($P<0.05$). Likewise, LB100 produced similar radiosensitization in pancreatic cancer cells, but minimal radiosensitization in normal small intestinal cells. Mechanistically, PPP2R1A siRNA or LB100 caused aberrant CDK1 activation, likely resulting from accumulation of the active forms of PLK1 (pPLK1 T210) and CDC25C (pCDC25C T130). Furthermore, LB100 inhibited radiation-induced Rad51 focus formation and homologous recombination repair (HRR), ultimately leading to persistent radiation-induced DNA damage, as reflected by γH2AX expression. Finally, we identified CDC25C as a key PP2A substrate involved in LB100-mediated radiosensitization as depletion of CDC25C partially reversed LB100-mediated radiosensitization. In a mouse xenograft model of human pancreatic cancer, LB100 produced significant radiosensitization with minimal weight loss.

**Conclusions—**Collectively, our data demonstrate that PP2A inhibition radiosensitizes pancreatic cancer both *in vitro* and *in vivo* via activation of CDC25C/CDK1 and inhibition of HRR, and provide proof-of-concept evidence that PP2A is a promising target for the improvement of local therapy in pancreatic cancer.

### Keywords

pancreatic cancer; protein phosphatase 2A; radiosensitization; homologous recombination repair

Requests for reprints: Meredith A. Morgan, Department of Radiation Oncology, University of Michigan Medical School, Room 4326B Medical Sciences I, Ann Arbor, MI, 48109-5637, Phone: 734-647-5928, Fax: 734-763-1581, mmccrack@med.umich.edu.

**Disclosure of potential conflicts of interest:** None.

## Introduction

Pancreatic cancer remains one of the most difficult-to-treat cancers with a 5-year survival of less than 6%, representing the most lethal type of cancer in the United States (1). Although gemcitabine has been the standard systemic therapy in this malignancy, new therapies for metastatic disease, such as FOLFIRNOX and Abraxane plus gemcitabine are emerging (2, 3). However, for approximately 30% of pancreatic cancer patients local disease progression is the cause of mortality (4), highlighting the importance of local disease control. Intensification of therapy for locally advanced disease with concurrent radiation and gemcitabine results in improved survival (5–7). Despite these advancements, the median survival for patients with locally advanced disease, treated with chemoradiation ranges from 11 to 19 months, underscoring the need for further improvement of local disease therapy.

Previously, we have utilized a library of siRNA against protein kinases and E3 ubiquitin ligases to identify potential radiosensitizing targets in glioblastoma cells (8). On the basis of this drug target discovery platform, we performed a high-throughput siRNA library screen in human pancreatic cancer cells in an attempt to identify novel molecular targets whose silencing caused sensitization to the combination of gemcitabine and radiation. We identified PPP2R1A, a structural subunit of protein phosphatase 2A (PP2A) as a lead target that when depleted by siRNA enhanced the cytotoxicity of chemoradiation treatment (Suppl. Fig. 1). PP2A is a ubiquitous, multifunctional serine/threonine phosphatase that typically contains a catalytic (C), structural (A), and variable regulatory subunit (B). In humans, the C and A subunits are each encoded by two distinct genes (PPP2CA/Cα and PPP2CB/Cβ for C subunit; PPP2R1A and PPP2R1B for A subunit). The B subunit is divided into four unrelated families (B/B55/PR55, B′/B56/PR61/PPP2R5, B″/PR72/PPP2R3 and B‴/PR93/PR110) with at least 26 isoforms that control the substrate specificity of the PP2A heterotrimeric complex (9–11). The complexity of the PP2A complex within cells allows the enzyme to mediate diverse physiological functions. Its aberrant activity has been linked with several pathological conditions, notably cancer (9). Based on the role of PP2A in mediating the DNA damage response (12) and the prevalence of aberrations in the DNA damage response in cancer, inhibition of PP2A may further exacerbate DNA damage in cancer cells.

Pharmacological inhibition of PP2A produces anti-tumor activity against pancreatic cancer and other human cancer types highlighting PP2A as an attractive target for the development of novel anti-cancer drugs with an emphasis on cantharidin and norcantharidin analogues (13–17). Inhibition of PP2A sensitizes cancer cells to radiation and chemotherapy by mechanisms including sustained phosphorylation of p53, γH2AX, PLK1, AKT, Ku, and DNA-PKcs leading to apoptosis, cell cycle deregulation, and inhibition of DNA repair (13, 14, 18–21). PP2A also regulates CDC25C although it is not known what effect this imparts on sensitization to radiation or chemotherapy (22). Based on these mechanisms of action, PP2A is potentially a useful target for sensitization to radiation.

Given that previous studies investigating PP2A inhibition as a radiosensitizing strategy were conducted with siRNA or toxic small molecule inhibitors (e.g. okadaic acid), in the present study we investigated the novel pharmacological PP2A inhibitor, LB100, a clinical candidate agent currently entering Phase I clinical trials (13). While LB100 (and its homolog LB1.2) has been shown to sensitize to temozolomide and doxorubicin (14, 23), it remains to be determined if it has radiosensitizing activity. Since we identified PPP2R1A as a sensitizing target in our siRNA library screen, we compared radiosensitization by LB100 to PPP2R1A siRNA. We found that both LB100 and PPP2R1A siRNA produced similar and significant radiosensitization in pancreatic cancer cells. To determine the mechanism(s) of radiosensitization by PP2A inhibition, we assessed known PP2A substrates such as CDC25C, as well as DNA response and repair via analysis of γH2AX, RAD51, and an HRR

reporter assay. Finally, we tested the radiosensitizing efficacy and tolerability of LB100 in *in vivo* pancreatic tumor models.

## Materials and Methods

### Cell culture, siRNA, and drug solutions

Human pancreatic cancer cell lines MiaPaCa-2 and Panc-1 and the normal human small intestine epithelial cell line CCL-241 were obtained from American Type Culture Collection (ATCC) and grown in either DMEM medium (MiaPaCa-2 and Panc-1) with 10% fetal bovine serum (FBS) or HybriCare medium (ATCC) supplemented with 30 ng/ml epidermal growth factor and 10% FBS (CCL-241). Cell cultures were maintained in an atmosphere of 5% $CO_2$/95% air at 37°C and tested free of *Mycoplasma* contamination. Nonspecific, PPP2R1A, and CDC25C SMARTpool siRNAs (100nmol/L; Dharmacon) were delivered using X-tremeGENE transfection reagent (Roche) per the manufacturer's protocol. LB100 (for structure, see Suppl. Fig. 3A), a water-soluble homolog of LB102 that is a specific competitive small-molecule inhibitor of PP2A (versus PP1) (13, 24), was provided by Lixte Biotechnology Holdings, Inc.

### siRNA screen

Primary and confirmatory siRNA screens were performed with the Dharmacon siRNA library. This library includes siRNA oligonucleotides against 8800 'druggable' genes with 4 siRNAs per gene that have each been validated to silence their target mRNA up to 75%. MiaPaCa-2 cells plated in a 96-well format at 400 cells per well were transfected with the siRNA library (40nmol/L) using X-tremeGENE transfection reagent. Non-specific (si-NS), CHK1 and PLK1 -targeting SMARTpool siRNAs (Dharmacon) were included as negative and positive controls, respectively. Twenty-four hours post transfection, either gemcitabine (50 nmol/L) or vehicle (serum-free medium) was added to the wells for 2 hours, after which the medium was replaced with fresh growth medium with antibiotics. After additional incubation for 24 hours, the gemcitabine-treated cells were treated with 4Gy ionizing radiation (IR). Cell viability was determined 72 to 96 h post-IR with the ATPlite Kit (Perkin Elmer) according to the manufacturer's instructions. Radiation enhancement ratios were calculated by dividing the viability of si-NS+gemcitabine+IR-treated wells (normalized for si-NS toxicity) by the viability of specific siRNA+gemcitabine+IR-treated wells (normalized for specific siRNA toxicity). Using similar methodology, a secondary, confirmatory siRNA screen was performed; ultimately yielding a total of 69 identified and confirmed hits. Suppl. Fig. 1 illustrates the siRNA screening methodology and the top 15 hits.

### Clonogenic survival assay

Cells were seeded in 60-mm dishes at cloning densities in duplicate or triplicate and irradiated 72 h post-transfection with si-PPP2R1A, si-NS, or mock, followed by incubation at 37°C for 7–12 days. After fixation with 0.2% crystal violet, colonies containing more than 50 individual cells were counted. Survival curves were fitted using the linear-quadratic equation and mean inactivation dose was calculated as previously described (25). Radiation enhancement ratios (RER) were calculated as the ratio of the mean inactivation dose under control (Mock) conditions divided by the mean inactivation dose after either siRNA or LB100 treatment (26).

### Immunoblotting

Whole cell and homogenized tissue lysates were prepared in cold RIPA buffer (50 mmol/L Tris-HCl pH 7.5, 150 mmol/L NaCl, 2 mmol/L EDTA, 1% SDS, 0.2% Triton X-100 and

0.3% NP-40) supplemented with phosphatase (Roche) and protease inhibitors (Roche) as previously described (27). The following antibodies were used: PPP2R1A (Abcam), phospho-CDK1(Y15), phospho-PLK1 (T210) (Cell Signaling Technology), γH2AX (Millipore), WEE1, CDK1, CDC25C (Santa Cruz Biotechnology), β-actin (Sigma) and phospho-CDC25 (T130; a gift from S. Kornbluth, Duke University, Durham, NC).

### Flow Cytometry

Cells were trypsinized, washed with PBS, and fixed in ice-cold 70% ethanol. For γH2AX analysis, cells were incubated overnight at 4°C with γH2AX antibody (Millipore) diluted in PBS containing 1% FBS and 0.2% Triton X-100 (PBT). After centrifugation, cells were incubated for 1 hour with FITC–conjugated anti-mouse antibody (Sigma) diluted 1:100 in PBT. Samples were then rinsed with PBT buffer and stained with propidium iodide solution (BD) for analysis. In untreated, control samples a gate was arbitrarily set to define a region of positive staining for γH2AX of approximately 5%. This gate was then overlaid on the treated samples. For phospho-Histone H3 (S10) analysis, samples were processed as previously described (28). Samples were analyzed on a FACScan flow cytometer (Becton Dickinson) and quantified with FlowJo software (Tree Star).

### Immunofluorescence staining

For RAD51, γH2AX, or 53BP1 foci visualization, cells grown on coverslips were treated as indicated and fixed with a 4% paraformaldehyde solution as previously described (29, 30). Samples were then permeabilized with PBS containing 0.5% Triton X-100, blocked with 15% FBS in PBS and incubated in blocking buffer with primary antibody against either RAD51 (GeneTex), γH2AX (Millipore), or 53BP1 (Novus Biologicals), followed by incubation with Alexa Fluor 594 goat anti-mouse IgG or Alexa Fluor 488 goat anti-rabbit IgG (Invitrogen). Samples were mounted onto slides with Prolong Gold Antifade Reagent containing DAPI (Invitrogen). RAD51 foci were imaged with an Olympus FV500 confocal microscope (Olympus America) (60x objective) while γH2AX and 53BP1 foci were imaged with a fluorescent microscope (IX71, Olympus America) (40x objective) and a CoolSnapEZ camera (Photometrics).

### Homologous recombination repair analysis

MiaPaCa2 cells were transfected with a construct encoding the DR-GFP recombination substrate (29, 30) using SuperFect transfection reagent (Qiagen) according to the manufacturer's protocol. Stable clones were selected with puromycin. To measure HRR, double strand breaks were induced by adenoviral-mediated expression of the restriction enzyme I-SceI, which cleaves the DR-GFP gene. HRR of this break restores wild-type GFP expression. The model was validated with Rad51 siRNA which inhibited restoration of the GFP signal. Experiments were performed in a single clone selected for consistent GFP expression following adenoviral transfection. Cells were collected 46 hrs post-SceI adenoviral infection, and the extent of double strand break repair by HRR was quantified by flow cytometric analysis of GFP expression.

### PP2A phosphatase activity assay

Pancreatic cancer cells grown to 70% confluence in 100 mm-dishes were treated with LB100 as indicated. After treatment for 2 h, cells were washed twice with cold PBS (pH7.4) and then lysed in extraction buffer (20 mmol/L imidazole-HCl, 2 mmol/L EDTA, 2 mmol/L EGTA, pH7.0) supplemented with protease inhibitors (Roche) for 30 min on ice. Cell lysates were sonicated for 10 sec and centrifuged at 2,000 × g for 5 min. Supernatants containing 400 μg of protein were assayed with the PP2A Immunoprecipitation Phosphatase

Assay Kit (Millipore) according to the manufacture's protocol. PP2A activity in MiaPaCa-2 xenografts was determined using the conditions described above.

### Animal experiments

All animal experiments were carried out according to a protocol approved by the University Committee for Use and Care of Animals. Five million MiaPaCa-2 cells in a 1:1 mixture of 10% FBS-DMEM/Matrigel (BD Biosciences) were injected subcutaneously into both flanks of nude mice. When average tumor volume reached the size of approximately 120 $mm^3$, the mice were randomized and the treatment was initiated. LB100 (1.5 mg/kg, I.P.) and radiation (1.2 Gy/fraction) were given once a day, 5 days a week for 2 weeks. Radiation was delivered directly to the tumor with the rest of the animal shielded. For combination treatment, LB100 was given 2 hours prior to radiation. The growth of tumors (8 for control group, 12–16 for the other groups) was measured twice a week and average tumor volume (TV) was calculated according to the equation: $TV = (L \times W^2)/2$, where L and W are the longer and shorter dimensions of the tumor, respectively. Radiation was conducted in the University of Michigan Comprehensive Cancer Center Experimental Irradiation Core.

### Irradiation

Irradiations were carried out using a Philips RT250 (Kimtron Medical) at a dose rate of ~2Gy/minute in the University of Michigan Comprehensive Cancer Center Experimental Irradiation Core. Dosimetry was carried out using an ionization chamber connected to an electrometer system that is directly traceable to a National Institute of Standards and Technology calibration. For tumor irradiation, animals were anesthetized with isoflurane and positioned such that the apex of each flank tumor was at the center of a 2.4cm aperture in the secondary collimator, with the rest of the mouse shielded from radiation.

### Statistical analysis

For *in vitro* experiments, one-way ANOVA with a Tukey's post-test was used. For *in vivo* tumor growth studies, log-rank tests were conducted to compare tumor volume doubling/tripling times between treatment arms. Time to tumor volume doubling/tripling is defined as the earliest day on which the tumor volume is at least twice/thrice as large as on the first day of treatment. Statistical significance was defined as a two-sided $P$-value $<0.05$. A bayesian hierarchical changepoint (BHC) model was used to estimate tumor growth profiles, characterized by a pre-nadir regression rate, a regression period, a nadir volume, and a post-nadir regrowth rate (31). Tumor cell killing fraction and tumor growth delay were derived from the BHC model and compared between treatment arms as previously described (32). A feature is considered to be statistically significant if the 95% HPD (highest probability density) interval of the difference in that feature does not cover zero.

## Results

### PPP2R1A depletion radiosensitizes pancreatic cancer cells

To identify novel targets that modulate the sensitivity of pancreatic cancer cells to gemcitabine-based chemoradiation treatment, we performed an siRNA library screen in MiaPaCa-2 cells (Suppl. Fig. 1). Confirmed 'hits' were rank ordered by their magnitude of sensitization, and we found PPP2R1A, a structural subunit of PP2A, among the top 5 targets identified (which also included CHK1, PLA2G4B, GPR2, and ATR). To validate PPP2R1A as a novel target for radiosensitization, we performed clonogenic survival assays with PPP2R1A siRNA in MiaPaCa-2 and Panc-1 cells. Depletion of PPP2R1A resulted in a significant radiosensitization with enhancement ratios of 1.4 in both MiaPaCa-2 and Panc-1 cells (Fig. 1). Given the necessity of PPP2R1A in the assembly of the functional PP2A

holoenzyme (9), these data support the candidacy of PP2A as a radiosensitizing target in pancreatic cancer cells.

Since PP2A has been implicated in regulating DNA double strand break repair (19, 20, 33), we examined whether PPP2R1A knockdown would affect γH2AX, a marker of DNA double strand breaks. Using both flow cytometry (Figs. 2A, B) and immunoblotting (Fig. 2C), we found that PPP2R1A depletion caused persistent γH2AX expression in response to radiation (at 24 hours post-IR) in MiaPaCa2 cells compared to control cells treated with radiation alone. Combined treatment with PPP2R1A siRNA and radiation caused persistent γH2AX expression in both MiaPaCa-2 and Panc-1 cells, as measured by immunoblotting (Fig. 2C). Given that PP2A functions as a negative regulator of CDK1 via inhibition of CDC25C (21, 34), we hypothesized that PPP2R1A siRNA would decrease pCDK1 (Y15; an inhibitory phosphorylation site) in response to radiation. Indeed, radiation alone caused pCDK1 (Y15) to increase, a state consistent with inhibition of CyclinB/CDK1 activity and G2 arrest. PPP2R1A siRNA either alone or in combination with radiation caused a reduction in pCDK1 levels which was associated with an increase in the percentage of mitotic cells (Suppl. Fig. 2). Collectively, these data suggest that depletion of PPP2R1A in pancreatic cancer cells interferes with the DNA damage response, which likely contributes to its radiosensitizing effects.

## LB100 sensitizes pancreatic cancer cells to radiation

Since disruption of the PP2A complex by PPP2R1A depletion radiosensitized both MiaPaCa-2 and Panc-1 cells, we went on to investigate the ability of the small molecule PP2A inhibitor, LB100, to radiosensitize pancreatic cancer cells. Consistent with previous findings (13), LB100 alone caused a concentration dependent decrease in PP2A enzymatic activity (Fig. 3A) and clonogenic survival (Suppl. Fig. 3), with a slightly greater effect in MiaPaCa-2 than Panc-1 cells. To determine the radiosensitizing efficacy of LB100, MiaPaCa-2 and Panc-1 cells were treated with relatively non-toxic concentrations of LB100 as illustrated (Fig. 3B). LB100 treatment resulted in significant radiosensitization in both cell lines, with RERs ranging from 1.2 to 1.4. To begin to determine whether radiosensitization following inhibition of PP2A might be tumor cell selective, we tested the ability of LB100 to radiosensitize a normal, small intestinal epithelial cell line, CCL-241. These cells are a relevant model for tumor cell selectivity as the duodenum is the dose limiting tissue for radiation treatment of pancreatic cancer. In contrast to pancreatic cancer cells, treatment of normal cells with LB100 (1 or 3 μmol/L) produced little to no radiosensitization (Suppl. Fig. 4). Taken together, these results suggest that LB100 selectively sensitizes pancreatic cancer cells to radiation.

## LB100 causes CDK1 activation in pancreatic cancer cells

To begin to determine the mechanisms responsible for LB100-mediated radiosensitization, we assessed known PP2A substrates involved in the DNA damage response, PLK1 and CDC25C, as well as their downstream effector, CDK1. PP2A functions as a negative regulator of PLK1 and CDC25C by removing phosphorylations (T210 and T130, respectively) required for activity, ultimately resulting in persistent Y15 phosphorylation of CDK1 (and to a lesser extent T14 phosphorylation) and G2 arrest in response to DNA damage (Fig. 4A) (21, 34–37). By inhibiting PP2A, we hypothesized that LB100 would activate CDC25C and/or PLK1 activity, resulting in activation of CDK1. Consistent with this hypothesis, we found that pPLK1 (T210) was increased by LB100 alone or in combination with radiation in MiaPaCa-2 and Panc-1 cells (Fig. 4B). Likewise, combined LB100 and radiation treatment caused an increase in pCDC25C (T130), although the effect of LB100 alone on pCDC25C (T130) was variable between the two cell lines. Given that PLK1 and CDC25C are both positive regulators of CDK1, we expected that accumulation of

the active forms of these enzymes (T210 and T130, respectively) would be associated with an increase in CDK1 activity (reflected by a decrease in CDK1 phosphorylation at Y15). Indeed, treatment with LB100 in the presence or absence of radiation led to a decrease in Y15 phosphorylation on CDK1 (Fig. 4B). Interestingly, we found that LB100 treatment also led to a decrease in WEE1 protein levels (Fig. 4B). This change may result from a feedback loop between PLK1 and/or CDK1 leading to WEE1 phosphorylation and subsequent ubiquitin-mediated proteosomal degradation (38). Taken together, these data demonstrate a series of molecular changes in response to inhibition of PP2A by LB100 which likely result in activation of CDK1.

## Inhibition of HRR by LB100 correlates with persistent DNA damage

The observed changes in CDC25C, PLK1, WEE1, and CDK1 suggest at least two possible mechanisms that may contribute to LB100-mediated radiosensitization. First, based on the well-established role of CDK1 in mitotic entry, LB100 may promote aberrant entry into mitosis following radiation (39). Second, because PP2A, WEE1, and CDK1 have recently been implicated in regulation of HRR (33, 40), we hypothesized that inhibition of PP2A by LB100 may also inhibit HRR. To distinguish between these two possibilities, we first examined levels of the mitotic marker pHistoneH3 (Ser10) in cells treated with LB100 and radiation. Although LB100 treatment alone caused an increase in the percentage of cells entering mitosis, there was no obvious interaction between LB100 and radiation on mitotic entry (Suppl. Fig. 5). On the other hand, in a previously described reporter assay for homology-directed repair of DNA double strand breaks (30), LB100 significantly inhibited HRR in irradiated cells (Fig. 4C). Furthermore, LB100 significantly inhibited radiation-induced RAD51 focus formation (Fig. 4D).

Given our finding that PPP2R1A depletion interferes with the DNA damage response (Fig. 2), we hypothesized that HRR suppression by the combination of LB100 and radiation would also correlate with persistent DNA damage. To test this hypothesis, we measured γH2AX levels in cells treated with radiation, LB100 or the combination, by both immunoblot and immunofluorescent staining. As shown in Figure 4E, γH2AX levels were higher in the combination treatment group than in cells treated with either radiation or LB100 alone. In addition, more γH2AX foci-positive cells were consistently observed in the combination treatment group than in cells treated with radiation alone (Suppl. Fig. 6). In order to rule out the possibility that the observed increase in γH2AX was a result of direct modulation of γH2AX by PP2A (19), we assessed 53BP1 focus formation, an independent marker of DNA double strand breaks (41). Similar to γH2AX, we found that LB100 caused an increase 53BP1 focus formation in response to radiation in MiaPaCa-2 and Panc-1 cells (Suppl. Fig. 7) thus confirming the presence of DNA double strand breaks. Taken together, these results suggest that LB100 inhibits HRR in irradiated cells, ultimately leading to persistent DNA damage.

## CDC25C depletion partially reverses LB100-mediated radiosensitization

The CDC25C phosphatase positively regulates CDK1 activity by removing the inhibitory phosphorylation at Y15. Based on our observation that the active form of CDC25C (pCDC25C (T130)) increased as a consequence of LB100 treatment, we hypothesized that CDC25C may play a critical role in LB100-mediated radiosensitization. We reasoned that if CDC25C activation is causal, then CDC25C inhibition should attenuate the radiosensitizing effects of LB100. Indeed, in MiaPaCa-2 cells, siRNA-based CDC25C silencing depleted CDC25C protein and restored pCDK1 (Y15) levels in response to LB100 treatment (Fig. 5A). More importantly, CDC25C silencing significantly suppressed LB100-induced radiosensitization (Fig. 5B, $P<0.05$). This rescue experiment clearly demonstrated that CDC25C plays, at least in part, a causal role in LB100-mediated radiosensitization.

### LB100 radiosensitizes pancreatic cancer in an *in vivo* xenograft tumor model

Finally, we investigated the radiosensitizing activity of LB100 using an *in vivo* MiaPaCa-2 xenograft model. We first defined the time-frame in which LB100 caused a maximal inhibition of PP2A activity in tumor tissues. As shown in Figure 6A, the greatest inhibition of PP2A activity (~20%) was achieved 2 hours post-administration of LB100 (1.5 mg/kg). We therefore chose an *in vivo* treatment schedule in which LB100 was administered 2 hours pre-irradiation. We treated tumor-bearing mice with LB100 and/or radiation for five consecutive days per week for two weeks in a manner similar to clinical radiation fractionation schedules. We found that treatment with LB100 alone had a modest, yet significant effect on tumor growth, extending the time required for tumor volume doubling from 8.5 days in vehicle-treated animals to 12.5 days ($P<0.05$; Fig. 6B-C). Radiation treatment also significantly delayed tumor growth and produced a 15.5 day delay in the time required for tumor volume doubling relative to vehicle-treated animals. More importantly, LB100 in combination with radiation produced the greatest effects on tumor growth resulting in 25 and 9.5 day delays in tumor volume doubling relative to vehicle- or radiation-treated groups, respectively. Tumor radiosensitization by LB100 was also evidenced by statistically significant differences determined by the BHC statistical model in the tumor regression period (95% HPD interval of the difference: 0.1–19.4 days), tumor cell killing fraction (95% HPD interval of the difference: 6%-70%), and tumor growth delay (95% HPD interval of the difference: 4.2–26.3 days). The combination of LB100 and radiation was well tolerated in mice and produced minimal (<10%) weight loss (Suppl. Fig. 8). Thus, LB100 is a potent radiosensitizer in this *in vivo* pancreatic cancer xenograft model.

To assess the molecular mechanisms associated with LB100 radiosensitization *in vivo*, we examined pCDC25C (T130) and pCDK1 (Y15) in MiaPaCa-2 xenografts following treatment with a single dose of LB100 and radiation. We found a small increase in pCDC25C levels in MiaPaCa-2 tumors in response to LB100 alone or in combination with radiation, although the magnitude of this response was variable between tumors (Fig. 6D). Consistent with this increase in pCDC25C (T130), we observed a decrease in pCDK1 (Y15) levels and an increase in γH2AX levels. Taken together, our results demonstrate that LB100 is an effective and tolerable agent for sensitizing pancreatic tumors to radiation therapy and acts, at least in part, by modulating CDC25C and CDK1.

## Discussion

Through an unbiased siRNA library screen, we have identified PPP2R1A, a subunit of the PP2A holoenzyme, as a potent sensitizing target in pancreatic cancer cells. We found that inactivation of PP2A via genetic (siRNA silencing) or pharmacological (LB100) approaches sensitized pancreatic cancer cells to radiation. Our mechanistic studies revealed that PP2A inhibition caused an accumulation of the active forms of PLK1 and CDC25C which corresponded to an increase in the active form of CDK1. We further demonstrated that LB100 inhibits HRR in irradiated cells. Given the excitement in the oncology community toward the development of HRR inhibitors as a novel class of anticancer agents (30, 33, 40, 42–44), our data are of importance in that they demonstrate that inhibition of PP2A results in impaired HRR, suggesting that PP2A inhibition may be efficacious not only in combination with radiation but likely with other molecularly targeted or DNA damaging agents.

Several previous studies have utilized both genetic and pharmacologic approaches to demonstrate that PP2A inhibition can sensitize tumor cells to both radiation and chemotherapy (13, 18, 45). The development of pharmacological inhibitors of PP2A, however, has been limited by the intrinsic toxicity of these agents. For many years, cantharidin, a natural product isolated from blister beetles in Chinese medicine, has been

investigated for its anti-cancer properties as well as its ability to inhibit PP2A (46). Give the high cytotoxicity of cantharidin, extensive effort has been made to develop less toxic derivatives, such as LB100. Thus far, inhibition of PP2A with LB100 has not produced substantial toxicity in animal models (23, 24).

Since PP2A is a ubiquitously expressed enzyme, understanding how inhibition of this phosphatase may selectively sensitize cancer cells (versus normal cells) to radiation or chemotherapy remains a key issue. Given that cancer cells often contain aberrations in their DNA damage response machinery (both DNA damage repair- and cell cycle- related), and that PP2A regulates many of these proteins, it is conceivable that deregulation of the DNA damage response by PP2A inhibition would be more detrimental to cancer cells than normal cells (12, 47). In addition, endogenous DNA damage related to oncogene expression likely renders cancer cells more vulnerable than normal cells to inhibition of the DNA damage response (48). Furthermore, because tumor cells are often aberrant in their G1 checkpoint, where DNA repair by non-homologous end-joining mainly occurs, they have an increased reliance on HRR for repair of DNA double-strand breaks (49). Thus, inhibition of HRR by LB100 may represent an additional tumor-cell-selective sensitizing mechanism. Indeed, we found that normal small intestinal cells were less radiosensitized by LB100 than pancreatic cancer cells and that the combination of LB100 with radiation produced a minimal toxicity in mice.

PP2A exerts phosphatase activity on an array of proteins involved in the DNA damage response including DNA-PKcs, CHK1, CHK2, CDC25C, γH2AX, PLK1, and p53 (12). When we investigated potential PP2A substrates involved in LB100-mediated radiosensitization, we found that LB100 caused accumulation of the active forms of both CDC25C and PLK1. PP2A negatively regulates CDC25C by dephosphorylation of T130, which facilitates 14-3-3 binding to CDC25C, cytosolic sequestration of CDC25C and ultimately inactivation of CDK1 (47). PLK1 is also negatively regulated by PP2A which further facilitates CDK1 inactivation via diminished CDC25C T130 phosphorylation and increased WEE1-mediated phosphorylation of CDK1 on Y15 (Fig. 4A) (38, 50). Although CDC25C is a known PP2A substrate, what role CDC25C played in radiosensitization by PP2A inhibition was not known. Thus, we tested whether CDC25C was a key downstream protein, responsible for LB100-mediated radiosensitization, and found in a rescue experiment that LB100-radiosensitization can be partially abrogated in pancreatic cells with CDC25C depletion.

The finding that CDC25C depletion only partially rescues cells from LB100-mediated radiosensitization suggests the involvement of other PP2A substrates, such as γH2AX. In a previous study, persistent phosphorylation of H2AX following inhibition of PP2A led to impaired DNA damage repair (19). Thus one possible interpretation of our data showing persistent γH2AX in response to PP2A inhibition and radiation (Figs. 2, 4, and 6) is that it is not only a consequence of DNA damage resulting from CDC25C/CDK1 activation and HRR inhibition, but also a partial cause of the DNA damage, as persistent H2AX phosphorylation itself has been shown to impede DNA double strand break repair. While we did confirm the presence of persistent DNA double strand breaks in response to LB100 and radiation by an independent method (53BP1 focus formation), still a causative role for γH2AX in the persistent damage cannot be excluded. Nevertheless, our radiosensitization data (Fig. 5) do suggest an important role for CDC25C in LB100-mediated radiosensitization.

Given our observation that G2 checkpoint abrogation was not a major mechanism of radiosensitization by LB100 (Suppl. Fig. 6), we went on to investigate the effects of LB100 on radiation-induced DNA damage repair pathways. Based on previous studies implicating

forced activation of CDK1 in HRR inhibition (via disruption of BRCA2-RAD51 interaction) (40, 51), as well as those connecting PP2A to HRR via regulation of BRCA1 and RAD51 (33), we hypothesized that LB100 might radiosensitize cells via inhibition of HRR. Indeed, we found that LB100 inhibited HRR as measured by both a GFP-based HRR reporter assay and a RAD51 focus formation assay. To our knowledge, this is the first study demonstrating HRR inhibition as a mechanism of radiosensitization by PP2A inhibition. It is possible that activation of CDK1 caused by PP2A inhibition plays a role in this HRR inhibition, and it will be important in future studies to further elucidate the molecular mechanisms by which LB100 inhibits HRR.

The data presented in this study provide the first preclinical evidence that a clinical candidate, small molecule inhibitor of PP2A is a radiosensitizing agent in pancreatic cancer cells. In order to further develop PP2A inhibitors such as LB100 it will be imperative to carefully examine the mechanisms of tumor cell selectivity as well as normal tissue toxicities. In addition, the results of recently initiated Phase I testing will be instructive in the safety and tolerability of LB100 in humans. In the context of HRR inhibition by LB100, it will also be of interest to explore the efficacy of LB100 in combination with other therapies such as PARP1 inhibitors as well as with chemoradiation regimens. The results of this study lay the preclinical foundation for the future development of PP2A inhibitors as a novel class of radiosensitizing agents.

## Supplementary Material

Refer to Web version on PubMed Central for supplementary material.

## Acknowledgments

**Grant support:** This work was funded by NIH Grants R01CA163895 (to MM), R01CA156744 (to YS), P50CA130810 (to TSL), and an Alfred B. Taubman Scholarship (to TSL).

## Abbreviations

| | |
|---|---|
| **DSB** | DNA double-strand break |
| **RER** | radiation enhancement ratio |
| **HRR** | homologous recombination repair |
| **IR** | ionizing radiation |
| **PBT** | Phosphate Buffered Saline with 0.2% Triton X-100 |
| **PP2A** | protein phosphatase 2A |
| **SF** | surviving fraction |
| **TV** | tumor volume |

## References

1. Siegel R, Naishadham D, Jemal A. Cancer statistics, 2012. CA Cancer J Clin. 2012; 62:10–29. [PubMed: 22237781]
2. Conroy T, Desseigne F, Ychou M, Bouche O, Guimbaud R, Becouarn Y, et al. FOLFIRINOX versus gemcitabine for metastatic pancreatic cancer. N Engl J Med. 2011; 364:1817–25. [PubMed: 21561347]
3. Von Hoff DD, Ramanathan RK, Borad MJ, Laheru DA, Smith LS, Wood TE, et al. Gemcitabine plus nab-paclitaxel is an active regimen in patients with advanced pancreatic cancer: a phase I/II trial. J Clin Oncol. 2011; 29:4548–54. [PubMed: 21969517]

4. Iacobuzio-Donahue CA, Fu B, Yachida S, Luo M, Abe H, Henderson CM, et al. DPC4 gene status of the primary carcinoma correlates with patterns of failure in patients with pancreatic cancer. J Clin Oncol. 2009; 27:1806–13. [PubMed: 19273710]
5. Ben-Josef E, Schipper M, Francis IR, Hadley S, Ten-Haken R, Lawrence T, et al. A Phase I/II Trial of Intensity Modulated Radiation (IMRT) Dose Escalation With Concurrent Fixed-dose Rate Gemcitabine (FDR-G) in Patients With Unresectable Pancreatic Cancer. Int J Radiat Oncol Biol Phys. 2012
6. Crane CH, Varadhachary GR, Yordy JS, Staerkel GA, Javle MM, Safran H, et al. Phase II trial of cetuximab, gemcitabine, and oxaliplatin followed by chemoradiation with cetuximab for locally advanced (T4) pancreatic adenocarcinoma: correlation of Smad4(Dpc4) immunostaining with pattern of disease progression. J Clin Oncol. 2011; 29:3037–43. [PubMed: 21709185]
7. Loehrer PJ Sr, Feng Y, Cardenes H, Wagner L, Brell JM, Cella D, et al. Gemcitabine alone versus gemcitabine plus radiotherapy in patients with locally advanced pancreatic cancer: an eastern cooperative oncology group trial. J Clin Oncol. 2011; 29:4105–12. [PubMed: 21969502]
8. Zheng M, Morgan-Lappe SE, Yang J, Bockbrader KM, Pamarthy D, Thomas D, et al. Growth inhibition and radiosensitization of glioblastoma and lung cancer cells by small interfering RNA silencing of tumor necrosis factor receptor-associated factor 2. Cancer Res. 2008; 68:7570–8. [PubMed: 18794145]
9. Eichhorn PJ, Creyghton MP, Bernards R. Protein phosphatase 2A regulatory subunits and cancer. Biochim Biophys Acta. 2009; 1795:1–15. [PubMed: 18588945]
10. Janssens V, Goris J. Protein phosphatase 2A: a highly regulated family of serine/threonine phosphatases implicated in cell growth and signalling. Biochem J. 2001; 353:417–39. [PubMed: 11171037]
11. Janssens V, Longin S, Goris J. PP2A holoenzyme assembly: in cauda venenum (the sting is in the tail). Trends in biochemical sciences. 2008; 33:113–21. [PubMed: 18291659]
12. Lee DH, Chowdhury D. What goes on must come off: phosphatases gate-crash the DNA damage response. Trends Biochem Sci. 2011; 36:569–77. [PubMed: 21930385]
13. Lu J, Kovach JS, Johnson F, Chiang J, Hodes R, Lonser R, et al. Inhibition of serine/threonine phosphatase PP2A enhances cancer chemotherapy by blocking DNA damage induced defense mechanisms. Proceedings of the National Academy of Sciences. 2009; 106:11697–702.
14. Martiniova L, Lu J, Chiang J, Bernardo M, Lonser R, Zhuang Z, et al. Pharmacologic modulation of serine/threonine phosphorylation highly sensitizes PHEO in a MPC cell and mouse model to conventional chemotherapy. PLoS One. 2011; 6:e14678. [PubMed: 21339823]
15. Li W, Chen Z, Gong F-R, Zong Y, Chen K, Li D-M, et al. Growth of the pancreatic cancer cell line PANC-1 is inhibited by protein phosphatase 2A inhibitors through overactivation of the c-Jun N-terminal kinase pathway. European Journal of Cancer. 2011; 47:2654–64. [PubMed: 21958460]
16. Lewy D, Soenen D, Boger D. Fostriecin: chemistry and biology. Current medicinal chemistry. 2002; 9:2005–32. [PubMed: 12369868]
17. Deng L, Dong J, Wang W. Exploiting Protein Phosphatase Inhibitors Based on Cantharidin Analogues for Cancer Drug Discovery. Mini reviews in medicinal chemistry. 2013
18. Mi J, Bolesta E, Brautigan DL, Larner JM. PP2A regulates ionizing radiation-induced apoptosis through Ser46 phosphorylation of p53. Mol Cancer Ther. 2009; 8:135–40. [PubMed: 19139122]
19. Chowdhury D, Keogh M-C, Ishii H, Peterson CL, Buratowski S, Lieberman J. gamma-H2AX dephosphorylation by protein phosphatase 2A facilitates DNA double-strand break repair. Molecular cell. 2005; 20:801. [PubMed: 16310392]
20. Wang Q, Gao F, Wang T, Flagg T, Deng X. A nonhomologous end-joining pathway is required for protein phosphatase 2A promotion of DNA double-strand break repair. Neoplasia. 2009; 11:1012–21. [PubMed: 19794960]
21. Yan Y, Cao P, Greer P, Nagengast E, Kolb R, Mumby M, et al. Protein phosphatase 2A has an essential role in the activation of γ-irradiation-induced G2/M checkpoint response. Oncogene. 2010; 29:4317–29. [PubMed: 20498628]
22. Forester CM, Maddox J, Louis JV, Goris J, Virshup DM. Control of mitotic exit by PP2A regulation of Cdc25C and Cdk1. Proc Natl Acad Sci U S A. 2007; 104:19867–72. [PubMed: 18056802]

23. Zhang C, Peng Y, Wang F, Tan X, Liu N, Fan S, et al. A synthetic cantharidin analog for the enhancement of doxorubicin suppression of stem cell-derived aggressive sarcoma. Biomaterials. 2010; 31:9535–43. [PubMed: 20875681]
24. Lu J, Zhuang Z, Song DK, Mehta GU, Ikejiri B, Mushlin H, et al. The effect of a PP2A inhibitor on the nuclear receptor corepressor pathway in glioma. Journal of neurosurgery. 2010; 113:225–33. [PubMed: 20001590]
25. Fertil B, Dertinger H, Courdi A, Malaise E. Mean inactivation dose: a useful concept for intercomparison of human cell survival curves. Radiation research. 1984; 99:73–84. [PubMed: 6739728]
26. Morgan MA, Parsels LA, Kollar LE, Normolle DP, Maybaum J, Lawrence TS. The combination of epidermal growth factor receptor inhibitors with gemcitabine and radiation in pancreatic cancer. Clin Cancer Res. 2008; 14:5142–9. [PubMed: 18698032]
27. Wei D, Li H, Yu J, Sebolt JT, Zhao L, Lawrence TS, et al. Radiosensitization of human pancreatic cancer cells by MLN4924, an investigational NEDD8-activating enzyme inhibitor. Cancer research. 2012; 72:282–93. [PubMed: 22072567]
28. Morgan MA, Parsels LA, Parsels JD, Lawrence TS, Maybaum J. The relationship of premature mitosis to cytotoxicity in response to checkpoint abrogation and antimetabolite treatment. Cell Cycle. 2006; 5:1983–8. [PubMed: 16931916]
29. Pierce AJ, Johnson RD, Thompson LH, Jasin M. XRCC3 promotes homology-directed repair of DNA damage in mammalian cells. Genes Dev. 1999; 13:2633–8. [PubMed: 10541549]
30. Morgan MA, Parsels LA, Zhao L, Parsels JD, Davis MA, Hassan MC, et al. Mechanism of radiosensitization by the Chk1/2 inhibitor AZD7762 involves abrogation of the G2 checkpoint and inhibition of homologous recombinational DNA repair. Cancer Res. 2010; 70:4972–81. [PubMed: 20501833]
31. Zhao L, Morgan MA, Parsels LA, Maybaum J, Lawrence TS, Normolle D. Bayesian hierarchical changepoint methods in modeling the tumor growth profiles in xenograft experiments. Clin Cancer Res. 2011; 17:1057–64. [PubMed: 21131555]
32. Demidenko E. Three endpoints of in vivo tumour radiobiology and their statistical estimation. Int J Radiat Biol. 2010; 86:164–73. [PubMed: 20148701]
33. Kalev P, Simicek M, Vazquez I, Munck S, Chen L, Soin T, et al. Loss of PPP2R2A inhibits homologous recombination DNA repair and predicts tumor sensitivity to PARP inhibition. Cancer Res. 2012; 72:6414–24. [PubMed: 23087057]
34. Margolis SS, Perry JA, Forester CM, Nutt LK, Guo Y, Jardim MJ, et al. Role for the PP2A/B56delta phosphatase in regulating 14-3-3 release from Cdc25 to control mitosis. Cell. 2006; 127:759–73. [PubMed: 17110335]
35. Jang Y-J, Ji J-H, Choi Y-C, Ryu CJ, Ko S-Y. Regulation of Polo-like Kinase 1 by DNA Damage in Mitosis INHIBITION OF MITOTIC PLK-1 BY PROTEIN PHOSPHATASE 2A. Journal of Biological Chemistry. 2007; 282:2473–82. [PubMed: 17121863]
36. McGowan CH, Russell P. Human Wee1 kinase inhibits cell division by phosphorylating p34cdc2 exclusively on Tyr15. The EMBO journal. 1993; 12:75. [PubMed: 8428596]
37. Liu F, Stanton JJ, Wu Z, Piwnica-Worms H. The human Myt1 kinase preferentially phosphorylates Cdc2 on threonine 14 and localizes to the endoplasmic reticulum and Golgi complex. Molecular and cellular biology. 1997; 17:571–83. [PubMed: 9001210]
38. Watanabe N, Arai H, Nishihara Y, Taniguchi M, Watanabe N, Hunter T, et al. M-phase kinases induce phospho-dependent ubiquitination of somatic Wee1 by SCFβ-TrCP. Proceedings of the National Academy of Sciences of the United States of America. 2004; 101:4419–24. [PubMed: 15070733]
39. Malumbres M, Barbacid M. Cell cycle, CDKs and cancer: a changing paradigm. Nature Reviews Cancer. 2009; 9:153–66.
40. Krajewska M, Heijink AM, Bisselink YJ, Seinstra RI, Sillje HH, de Vries EG, et al. Forced activation of Cdk1 via wee1 inhibition impairs homologous recombination. Oncogene. 2012
41. Noon AT, Goodarzi AA. 53BP1-mediated DNA double strand break repair: insert bad pun here. DNA Repair (Amst). 2011; 10:1071–6. [PubMed: 21868291]

42. Vance S, Liu E, Zhao L, Parsels JD, Parsels LA, Brown JL, et al. Selective radiosensitization of p53 mutant pancreatic cancer cells by combined inhibition of Chk1 and PARP1. Cell cycle (Georgetown, Tex. 2011; 10:4321–9.
43. Ibrahim YH, Garcia-Garcia C, Serra V, He L, Torres-Lockhart K, Prat A, et al. PI3K inhibition impairs BRCA1/2 expression and sensitizes BRCA-proficient triple-negative breast cancer to PARP inhibition. Cancer Discov. 2012; 2:1036–47. [PubMed: 22915752]
44. Nowsheen S, Cooper T, Stanley JA, Yang ES. Synthetic lethal interactions between EGFR and PARP inhibition in human triple negative breast cancer cells. PLoS One. 2012; 7:e46614. [PubMed: 23071597]
45. Price WA, Stobbe CC, Park SJ, Chapman JD. Radiosensitization of tumour cells by cantharidin and some analogues. Int J Radiat Biol. 2004; 80:269–79. [PubMed: 15204704]
46. Shan HB, Cai YC, Liu Y, Zeng WN, Chen HX, Fan BT, et al. Cytotoxicity of cantharidin analogues targeting protein phosphatase 2A. Anticancer Drugs. 2006; 17:905–11. [PubMed: 16940800]
47. Bollen M, Gerlich DW, Lesage B. Mitotic phosphatases: from entry guards to exit guides. Trends Cell Biol. 2009; 19:531–41. [PubMed: 19734049]
48. Halazonetis TD, Gorgoulis VG, Bartek J. An oncogene-induced DNA damage model for cancer development. Science. 2008; 319:1352–5. [PubMed: 18323444]
49. Jeggo PA, Geuting V, Lobrich M. The role of homologous recombination in radiation-induced double-strand break repair. Radiother Oncol. 2011; 101:7–12. [PubMed: 21737170]
50. Franckhauser C, Mamaeva D, Heron-Milhavet L, Fernandez A, Lamb NJ. Distinct pools of cdc25C are phosphorylated on specific TP sites and differentially localized in human mitotic cells. PLoS One. 2010; 5:e11798. [PubMed: 20668692]
51. Zhang W, Peng G, Lin SY, Zhang P. DNA damage response is suppressed by the high cyclin-dependent kinase 1 activity in mitotic mammalian cells. J Biol Chem. 2011; 286:35899–905. [PubMed: 21878640]

## Statement of Translational Relevance

Intensification of local therapy through the use of radiation (in combination with chemotherapy) improves survival in patients with locally advanced pancreatic cancer. In order to further improve the efficacy of chemoradiation therapy in pancreatic cancer we sought to identify novel targets whose inhibition would sensitize pancreatic cancer cells to therapy. Identification and confirmation of PPP2R1A, a subunit of PP2A, as a radiosensitizing target led us to combine the small molecule PP2A inhibitor, LB100, currently entering Phase I clinical trials with radiation in pancreatic cancer. We found that LB100 sensitized pancreatic cancer cells and tumors to radiation, but produced only minimal sensitization of normal small intestinal cells with no observable toxicity in animals. Our study provides proof-of-concept evidence that PP2A inhibition is a promising strategy for selectively improving local therapy, and thus survival in pancreatic cancer.

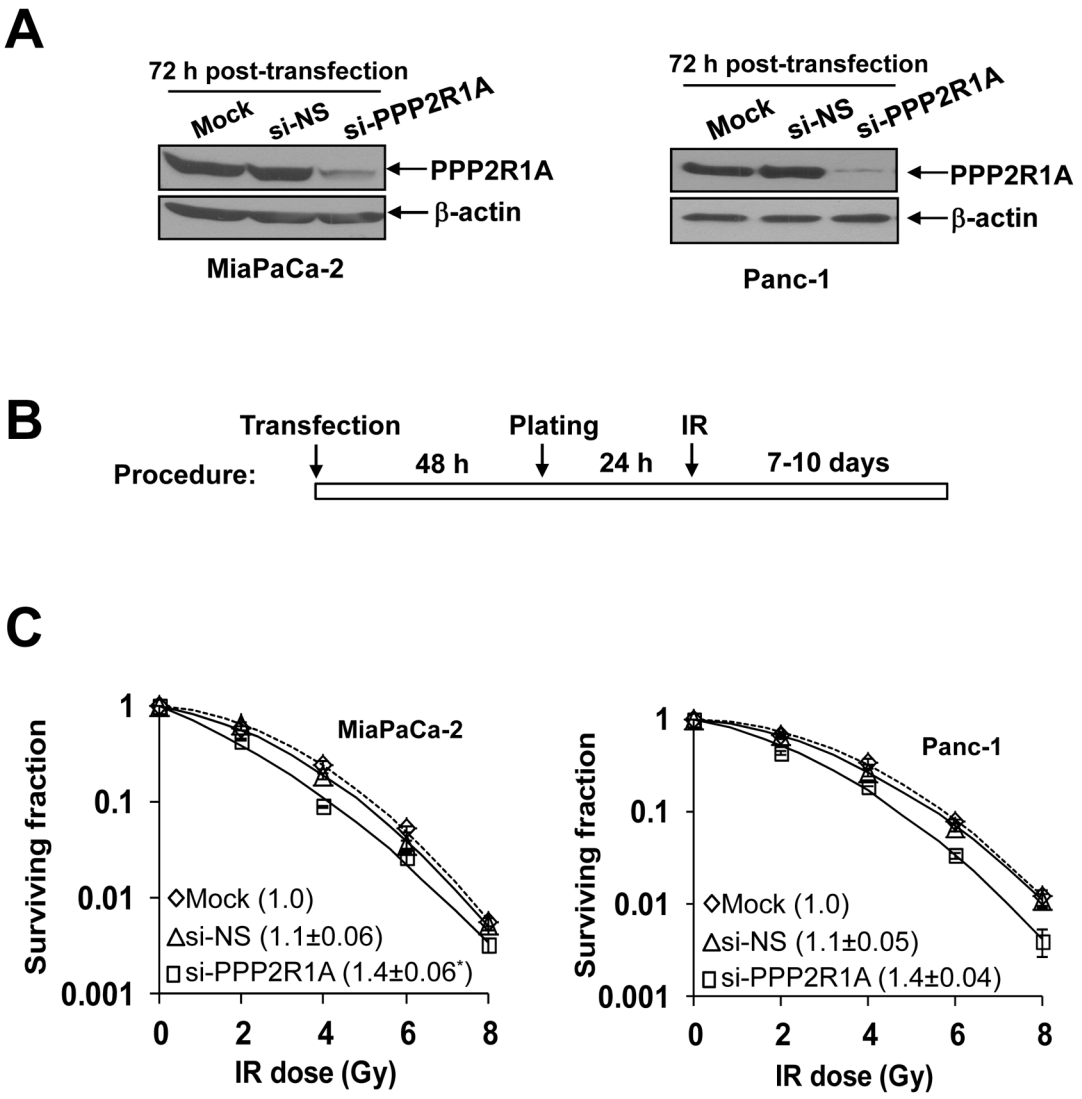


**Figure 1. PPP2R1A depletion radiosensitizes pancreatic cancer cells**

A, PPP2R1A protein levels in cells transfected with the indicated siRNA pools (100nmol/L). B, MiaPaCa-2 and Panc-1 cells treated as illustrated were assayed for clonogenic survival. Plots shown are representative of 2 – 3 independent experiments. Data in the legend are the mean radiation enhancement ratios (RER) ± SD (n = 2 – 3). The mean cytotoxicity of siRNA treatments was 1.0 (mock), 0.6 (siNS), and 0.6 (si-PPP2R1A) in MiaPaCa-2 and 1.0 (mock), 0.9 (si-NS), and 0.8 (si-PPP2R1A) in Panc-1 cells with less than 15% SD. Statistically significant differences in RER are indicated versus Mock*.

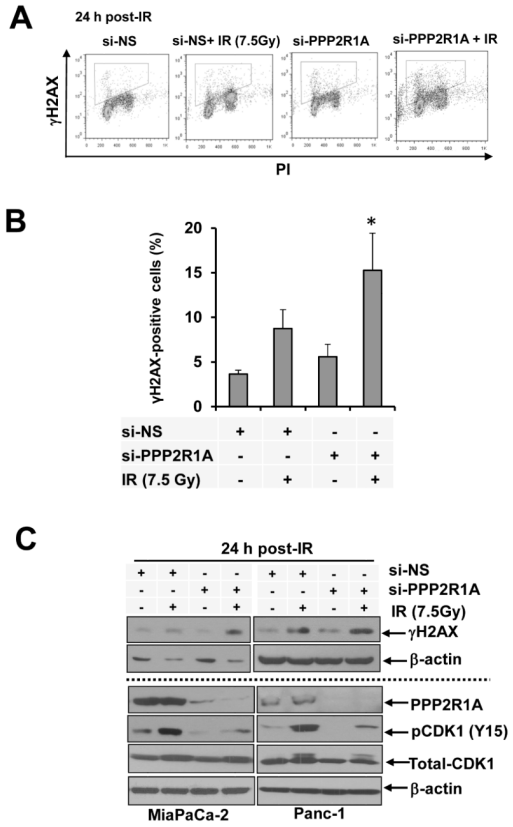


**Figure 2. PPP2R1A depletion leads to persistent radiation-induced DNA damage**

MiaPaCa-2 cells transfected with either si-PPP2R1A or si-NS were treated with radiation and collected 24 hours later for flow cytometric analysis of γH2AX (A, B) and immunoblot analysis of the indicated proteins (C). γH2AX-positive cells are defined by the gates shown (A). Data presented are the mean percentage of γH2AX positive cells ± SE (n = 3) and statistical significance versus IR* is indicated (B). Immunoblots are representative of at least 2 independent experiments.

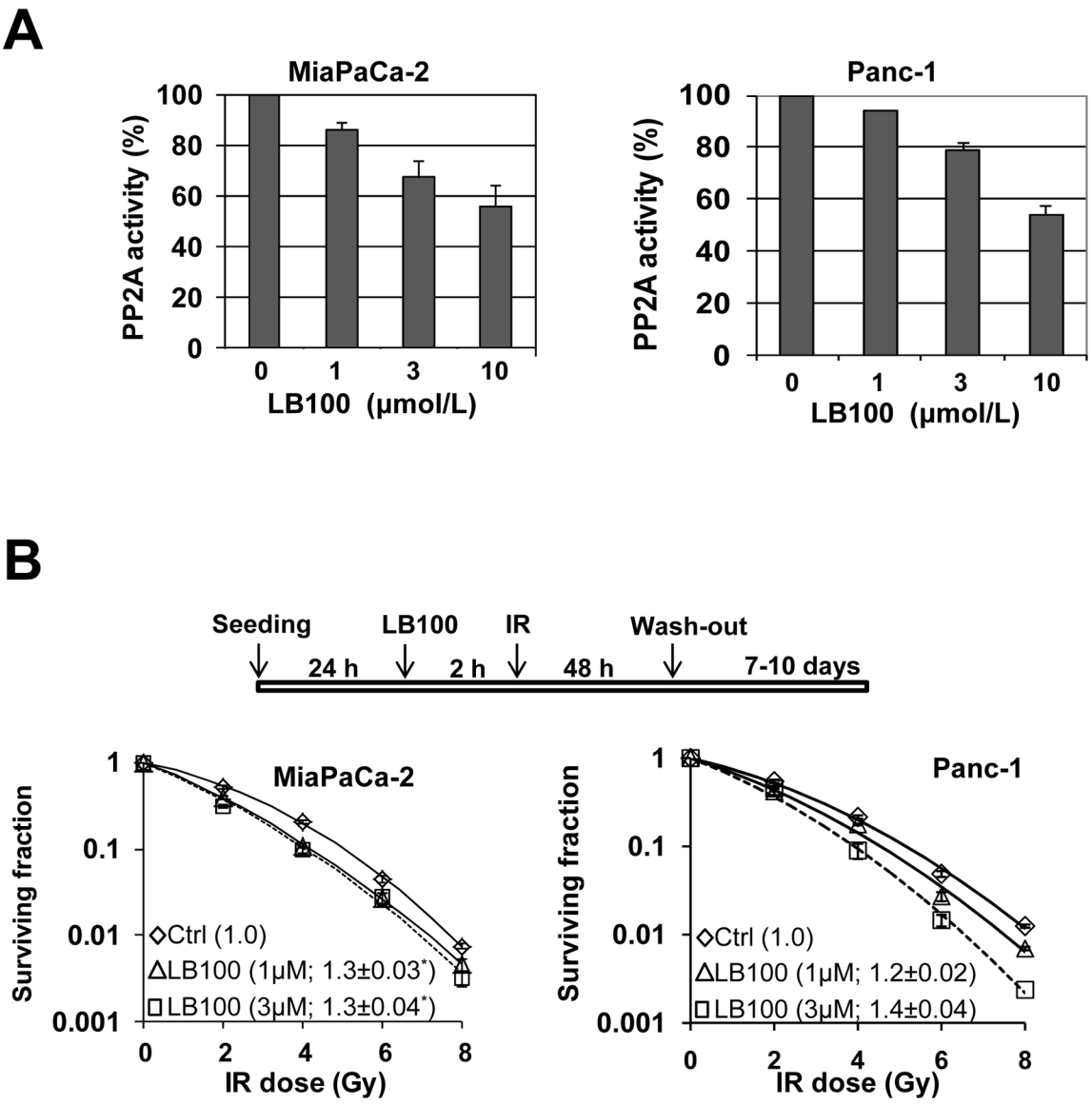


**Figure 3. Inhibition of PP2A by LB100 radiosensitizes pancreatic cancer cells**

A, MiaPaCa-2 and Panc-1 cells were treated with various concentrations of LB100, as indicated, for 2 hours. Cells were then harvested and PP2A activity was assayed as described in Materials and Methods. B, Cells were treated with 1 or 3 μmol/L LB100 and radiation as indicated and then assessed for clonogenic survival. Plots shown are representative of 2 – 3 independent experiments. Data in the legend are the mean RER ± SD (n = 2 – 3). The mean cytotoxicity of siRNA treatments was 1.0 (Ctrl), 0.9 (1uM), and 0.8 (3uM) in MiaPaCa-2 and 1.0 (Ctrl), 0.9 (1uM), and 0.7 (3uM) in Panc-1 cells with less than 10% SD. Statistically significant differences versus control* are indicated.

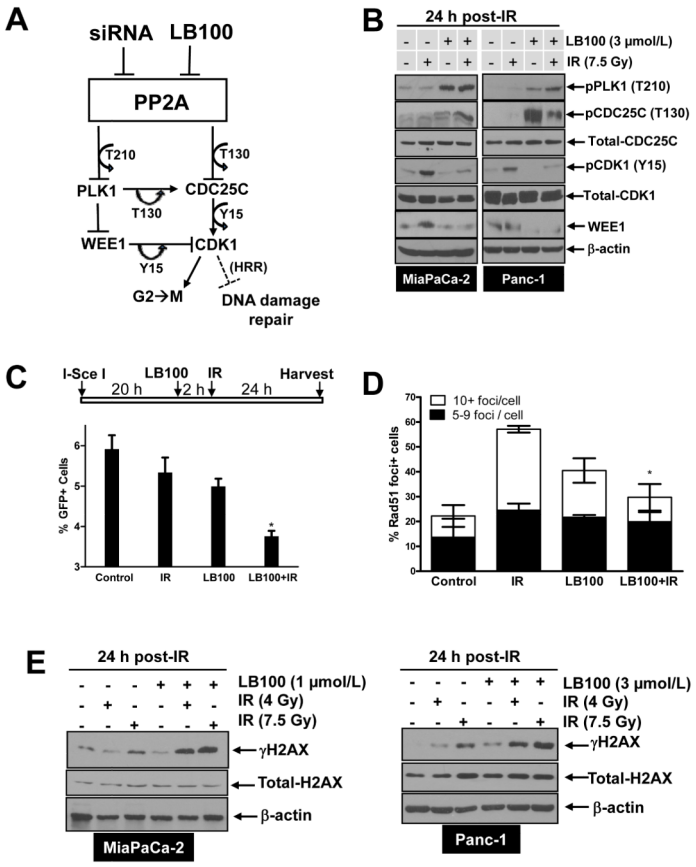


**Figure 4. Mechanisms of LB100-mediated radiosensitization**

A, Schematic diagram illustrating the consequences of PP2A inhibition. Inhibition of PP2A by siRNA or LB100 results in activation of PLK1 and CDC25C (via accumulation of T210 and T130 phosphorylations, respectively). Active PLK1 positively regulates CDC25C (T130) and negatively regulates WEE1, resulting in enhanced dephosphorylation of CDK1 (Y15) by CDC25C and impaired phosphorylation of CDK1 (Y15) by WEE1, leading to activation of CDK1. Active CDK1, together with cyclin B is the key regulator of the G2/M cell cycle transition. In addition, CDK1 may negatively regulate HRR. B, E, MiaPaCa-2 and Panc-1 cells were treated with LB100 for 2 hours pre- and 24 hours post-IR. At the end of treatment, cells were harvested for immunoblot analysis. C, MiaPaCa-2-DR-GFP cells were treated as illustrated and the percentage of GFP positive cells was measured by flow cytometry. Data are expressed as the mean percentage of GFP positive cells ± SE from 3 independent experiments. Statistical significance versus IR* is indicated. D, MiaPaCa-2 cells were treated as described in Fig. 4B and fixed for immunofluorescence 6 hours post-IR. Data are the mean percentage of Rad51 positive nuclei ± SE (n = 3). Statistical significance versus IR* is indicated (C, D).

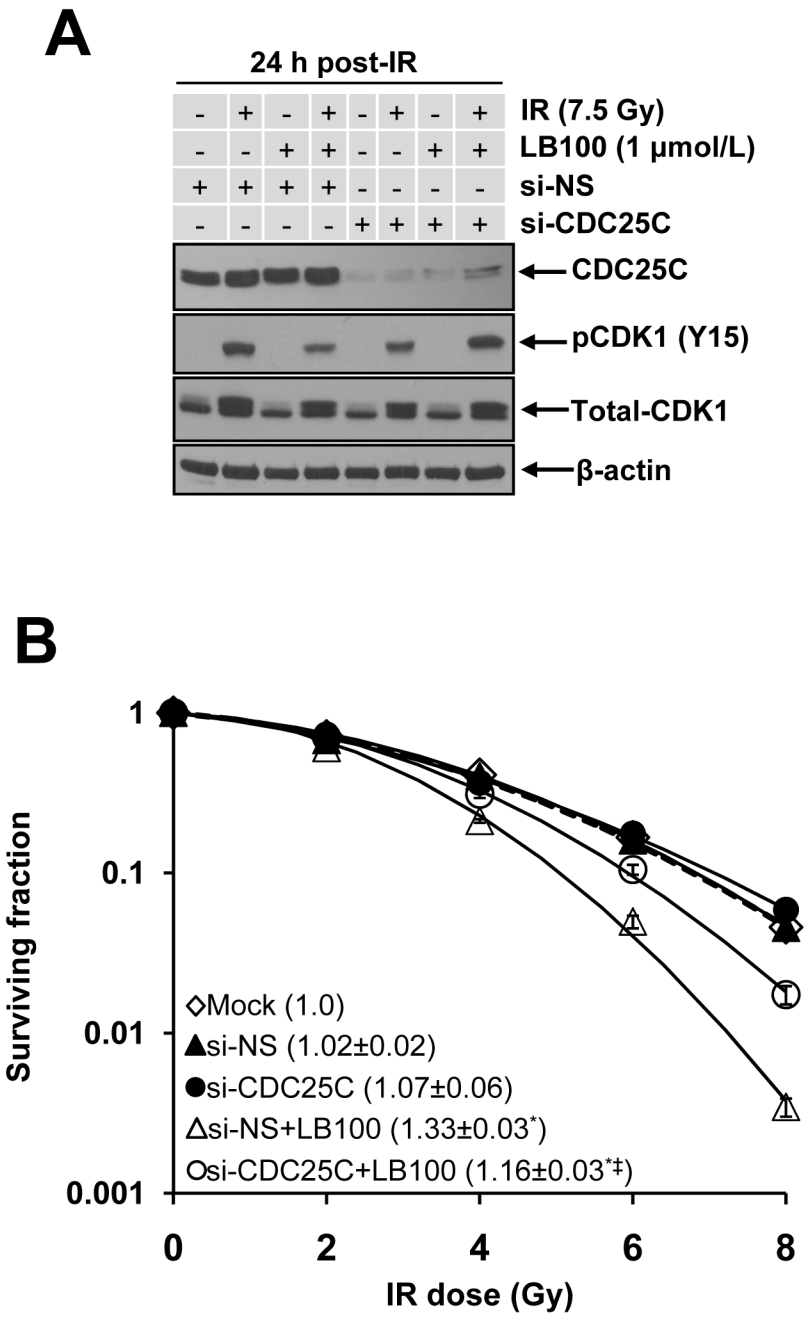


**Figure 5. LB100-mediated radiosensitization is partially rescued by CDC25C depletion**

A, MiaPaCa-2 cells were transfected with the indicated siRNA pools. Seventy-two hours post-transfection, cells were treated with LB100 for 2 hours pre- and 24 hours post-IR and harvested for immunoblotting for the indicated proteins. B, MiaPaCa-2 cells were transfected and plated for clonogenic survival as illustrated in Fig. 1B with the addition of LB100 2 hours pre- and 48 hours post-IR. Plots shown are representative of 3 independent experiments. Data in the legend are the mean RER ± SE (n = 3). The mean cytotoxicity of siRNA treatments was 1.0 (mock), 0.9 (si-NS), 0.7 (si-NS+LB100), 0.6 (si-CDC25C), and 0.5 (si-CDC25C+LB100) with less than 15% SE. Statistical significance versus Mock* or si-NS+LB100‡ is indicated.

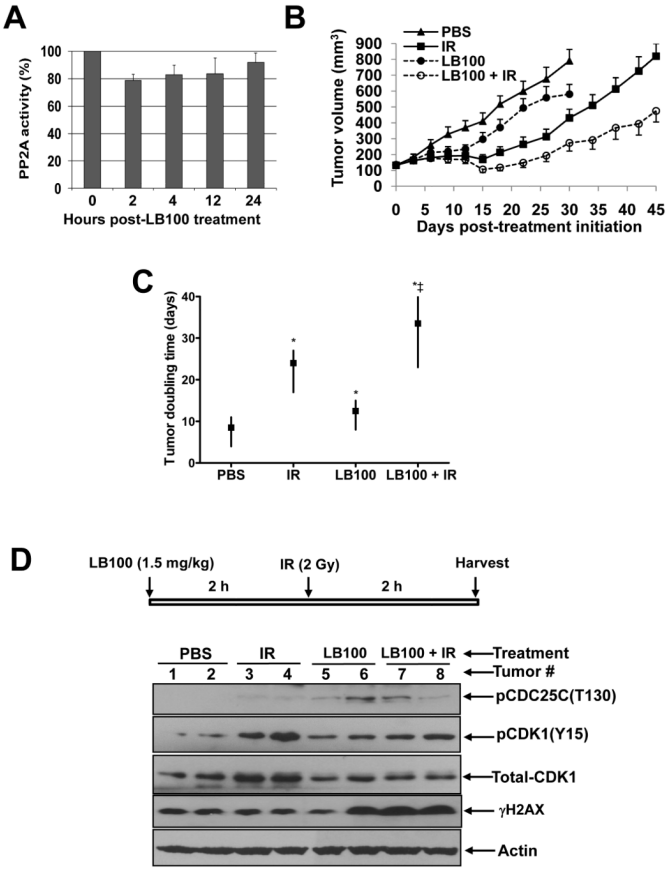


**Figure 6. Radiosensitization of MiaPaCa-2 xenografts by LB100**

A, Mice bearing MiaPaCa-2 xenografts (~200 $mm^3$) were treated with a single dose of LB100 (1.5 mg/kg). Tumors (n = 3 per group) were harvested at the indicated time points and assayed for PP2A activity. B and C, Mice bearing MiaPaCa-2, subcutaneous flank xenografts were randomized and treated with PBS (vehicle control), LB100 (1.5mg/kg; Mon-Fri, 2 hours pre-IR), and/or IR (1.2Gy/fraction; Mon-Fri) for 2 cycles. Tumor growth was monitored for 45 days or until the tumors reached approximately 7 times their starting volume, whichever occurred first. Data are the mean tumor volume ± SE obtained from 12 – 16 tumors per treatment condition (B) or are the median time required for tumor volume doubling with upper and lower limits of a 95% confidence interval (C). Statistically significant differences in tumor volume doubling are indicated versus PBS* and IR‡. D, Mice bearing MiaPaCa-2 xenografts (~200 $mm^3$) were treated with a single dose of LB100 and/or IR as illustrated. Tumors (n = 2 per treatment group) were harvested for immunoblotting.